Off-Axis Sawteeth and Double-Tearing Reconnection in Reversed Magnetic Shear Plasmas in TFTR

Z. Chang,[1] W. Park,[1] E. D. Fredrickson,[1] S. H. Batha,[2] M. G. Bell,[1] R. Bell,[1] R. V. Budny,[1] C. E. Bush,[1] A. Janos,[1] F. M. Levinton,[2] K. M. McGuire,[1] H. Park,[1] S. A. Sabbagh,[3] G. L. Schmidt,[1] S. D. Scott,[1] E. J. Synakowski,[1] H. Takahashi,[1] G. Taylor,[1] and M. C. Zarnstorff[1]

[1]*Plasma Physics Laboratory, Princeton University, Princeton, New Jersey 08543*
[2]*Fusion Physics and Technology, Torrance, California 90503*
[3]*Columbia University, New York, New York 10027*

(Received 29 April 1996)

Off-axis sawteeth are often observed in reversed magnetic shear plasmas when the minimum safety factor q is near or below 2. Fluctuations with $m/n = 2/1$ (m and n are the poloidal and toroidal mode numbers) appear before and after the crashes. Detailed comparison has been made between the measured T_e profile evaluation during the crash and a nonlinear numerical magnetohydrodynamics simulation. The good agreement between observation and simulation indicates that the off-axis sawteeth are due to a double-tearing magnetic reconnection process. [S0031-9007(96)01514-1]

PACS numbers: 52.35.Py, 52.30.Jb, 52.55.Fa, 52.65.Kj

Sawtooth magnetohydrodynamics (MHD) activity is commonly observed in tokamak experiments when the central safety factor q is below 1 and rises monotonically with minor radius. In recent reversed magnetic shear (RS) experiments [1] in the Tokamak Fusion Test Reactor (TFTR), another kind of sawtooth activity has been observed in plasmas with nonmonotonic q profiles or hollow plasma current profiles when $q(r) > 1$. Understanding these $q > 1$ sawteeth is important not only because it can help us explore magnetic reconnection physics, but also because it is closely related to present and future advanced tokamak research, which uses low or negative shear and $q > 1$ to attain high pressure stable plasmas with strong neoclassical bootstrap currents.

Figure 1 shows a typical RS discharge. The RS configuration is obtained by combining an early energetic neutral beam injection (prelude phase) and large current ramp rate [1]. During the high power heating phase, this discharge developed an enhanced reversed shear (ERS) [1] mode. Two sawtooth events are observed after the main heating phase. One is at 3.3 sec, during the low beam power phase, and another is at 3.75 sec, in the post-beam phase. The q profile up to $t = 2.5$ sec is from motional Stark effect (MSE) polarimetry [2] measurement. After that, the q profile is calculated by a transport code TRANSP [3] based on measured plasma profiles. The minimum q ($q_{\min}$) and central q (q_0) are shown in Fig. 1(b), which indicates that the q profile is reversed, i.e., $q_0 > q_{\min}$. The sawteeth occur when the $q_{\min}$ passes 2. They can be easily seen on the electron temperature evolution [Fig. 1(c)] measured by an electron-cyclotron-emission (ECE) diagnostic system. Time evolution of some other measured parameters is shown in Figs. 1(d)–1(f). A correlated negative spike in plasma loop voltage ($\sim$0.3 V) and reduction in plasma radius ($\sim$0.3 cm) are also observed. These sawteeth can appear in the nonenhanced RS phase as well as in the ERS phase. There are no great changes in the sawtooth activity with different plasma composition (deuterium only or deuterium-tritium).

Two types of $q(r) > 1$ sawteeth are observed on TFTR: an off-axis sawtooth, which is observed most commonly, and an on-axis sawtooth. Figure 2(a) (the first sawtooth in Fig. 1) shows the T_e fluctuation and profile behavior of the off-axis sawtooth. The central T_e does not immediately crash at the sawtooth event. We call this an "annular crash." Precursors around the inversion region are often observed. Mode analysis using magnetic coils and two toroidally separated ECE systems

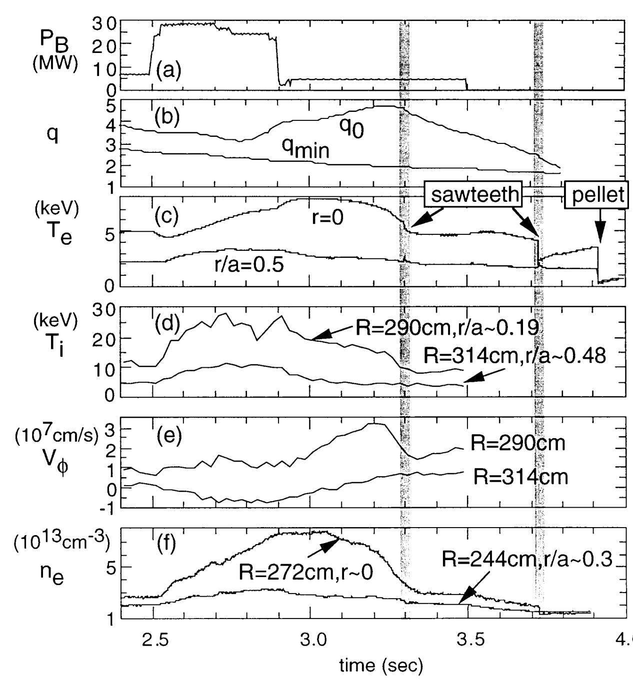

FIG. 1. Two sawtooth crashes were observed in this reversed shear discharge, one at 3.3 sec, the other at 3.72 sec. They occur after the $q_{\min}$ passes 2 (b). The correlated changes can be seen in T_e in (c), T_i in (d), V_ϕ in (e), and n_e in (f).

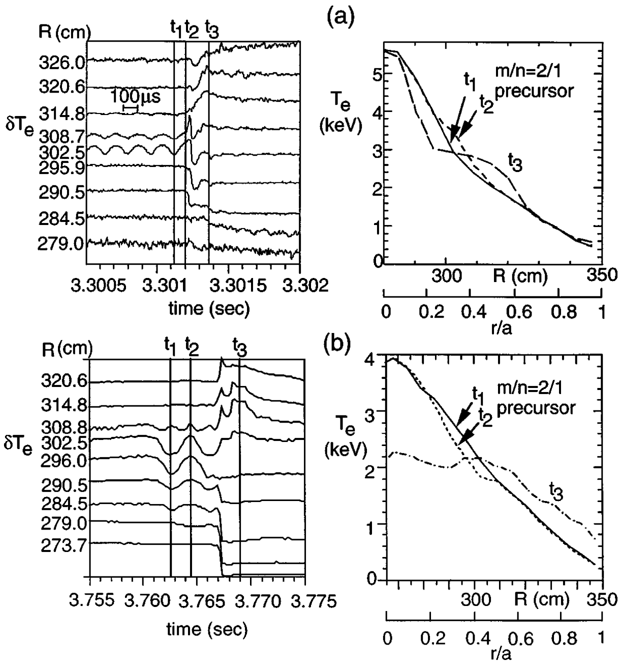

FIG. 2. Temperature fluctuations (left) and profile changes (right) for two kinds of sawtooth crashes. (a) Annular crash. Precursor with $m/n = 2/1$ is observed. The fast crash affects only the annular region. (b) Core crash. The $2/1$ precursor occupies a larger region.

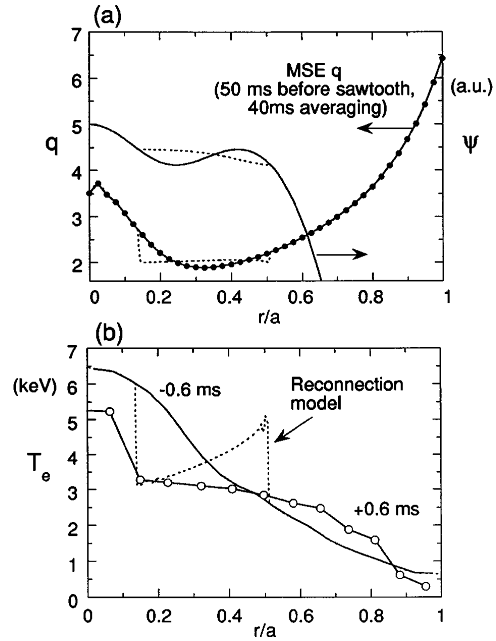

FIG. 3. Predicted profile changes after (dashed curves) a magnetic reconnection from the Kadomtsev model. The initial q and T_e profiles (solid curves) are taken from an off-axis sawtooth similar to the one in Fig. 2(a). ψ is the helical flux. The measured T_e after the sawtooth is also shown in (b).

[4] shows that the precursor mode has a toroidal mode number $n = 1$. The poloidal mode number is even from the phase analysis of the ECE data. The precursor (and postcursor when they exist) modes are identified as $m/n = 2/1$ modes since the q value near the MHD region is about 2, see Fig. 3(a). (Note that the external magnetic measurement usually gives $2 < m < nq_a$ due to toroidal coupling.) Figure 2(b) shows the second type of sawtooth (similar to the second sawtooth in Fig. 1). The central T_e crashes on nearly the same time scale (20–50 μsec) as the off-axis T_e crash. We call this case a "core crash." The $m/n = 2/1$ precursor mode occupies a larger region in the core-crash cases.

These observations (off-axis feature, fast time scale, and the multiple rational surfaces in the reversed q profile) suggest that the crashes are due to fast magnetic field line reconnection, analogous to a $q = 1$ reconnection. We find that the Kadomtsev model [5] applied to a double-tearing reconnection [6,7] qualitatively agrees with the observations. This theory assumes that, for a reversed shear magnetic configuration, two pairs of $m/n = 2/1$ islands develop at the two $q = 2$ surfaces and reconnect with a time scale much faster than the single-tearing case. Figure 3 shows the calculated changes of $q(r)$, helical magnetic flux ψ, and T_e before (from the measurement) and after the reconnection for an annular crash similar to the one shown in Fig. 2(a). The uncertainty on the q profile is typically about 10%. Here, in a cylindrical geometry we have $\psi(r) \propto \int_0^r (1/q - n/m) r dr$. After the reconnection, the q profile within the mixing region relaxes to ≥ 2. In large annular-crash sawteeth, changes in the magnetic pitch angles ($\sim 20\%$) are observed on the MSE channels in the vicinity of the sawtooth region, indicating an increase of q in the $q_{\min}$ region and a decrease of q in the mixing region. To date, only the changes in the inner mixing region ($r < r_{s1}$) have been observed. The T_e profile after the reconnection is usually strongly inverted due to the assumption of no transport during the reconnection. When the $q < 2$ region increases, the inner mixing radius becomes smaller and smaller. Eventually, when $\psi(r_{s2}) \geq \psi(r = 0) = 0$ or $\int_0^{r_{s2}} (1/q - n/m) r dr \geq 0$, the reconnection will cover the center. A core crash is then expected.

For a more detailed study, we used a nonlinear 3D MHD code MH3D [8] to follow the double-tearing reconnection process. Measured $T_e(r)$ and $q(r)$ from TRANSP before a sawtooth are used as initial conditions. The nonlinear development of the double-tearing instability is then followed self-consistently. The dominant behavior is the fast magnetic reconnection and subsequent T_e equalization along the reconnected field lines. The large parallel electron thermal conductivity is accurately treated using the technique of artificial parallel sound wave [9]. Here, we will present the result from a simulation of the second core-crash sawtooth in Fig. 1. For this relatively low beta case (volume averaged $\epsilon\beta_p \sim 0.03$), a 2D simulation gives a similar global behavior as 3D toroidal simulation which was carried out part way to check whether 3D toroidal effects are important. (For high-β cases, 3D toroidal effects often dominate the global behavior [8].) The Lundquist numbers $S \sim 10^4$ and 10^5 are used to ensure that the global behavior is not sensitive to the Lundquist number used, which is much lower than the experimental value of $S \sim 10^8$. Figure 4 shows the 2D simulation results using the plasma parameters for the core-crash case of the second sawtooth in Fig. 1. Four phases can be distinguished: (a) the early growth phase, (b) the double-tearing reconnection phase, (c) the central temperature (pressure) collapse phase, and (d) the final temperature (pressure) equalization phase. The left column of Fig. 4 displays the contours of the magnetic flux on a plasma cross section. The right column shows the corresponding T_e profiles in *minor radius.* For comparison, the T_e profile along the $\theta = 0°$ (O point of the inner island) is plotted on the right side. The T_e profile along the $\theta = 90°$ (O point of the outer island) is on the left side. At the early phase (a), the two pairs of islands are well separated. It is probably responsible for the observed $2/1$ precursor. At the reconnection phase (b), the inner hot islands move out through the X points of the outer cold islands. At the same time, the outer cold islands move in through the X points of the inner hot islands. Note that, since the reconnection time is much faster than the perpendicular transport time, the temperature profile around the 0° section is higher than the temperature around the 90° section, see Figs. 4(b) and 4(c). A relative "hot spot" appears at the outer mixing radius at the later stage of the reconnection, see Fig. 4(d). The reconnection time scale during the phases shown above corresponds to a Sweet-Parker scaling [10], $\tau_A^{1/2}\tau_R^{1/2}$, which is $\sim$1 msec for the experimental parameters [11]. While the experimental evolution time during the phase corresponding to (d) (see the next paragraph) roughly agrees with this, the experimental crash time corresponding to phases (b) and (c) is about an order of magnitude faster, possibly due to turbulence in the reconnection layer [12], which is not intended to be resolved in our calculation. What is contained in the global simulation is that the reconnection is much faster than the usual nonlinear tearing mode time scale ($\propto \tau_R$) of $\sim$100 msec for the experimental parameters studied here.

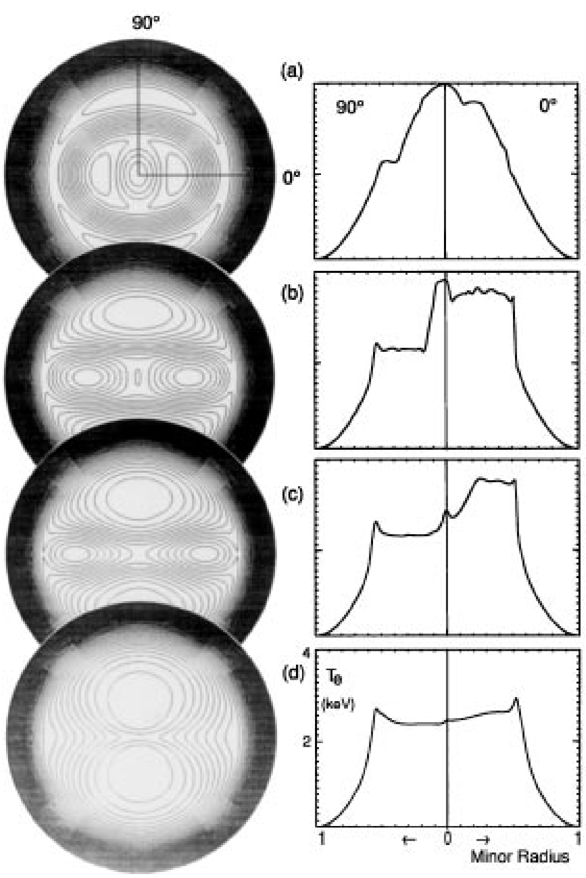

FIG. 4. Numerical simulation of a double-tearing reconnection. The left column shows the contours of the magnetic flux. The corresponding T_e profiles (in minor radius) for $\theta = 0°$ and 90° sections are shown on the right. Four phases can be distinguished: (a) the early growth phase, (b) the double-tearing reconnection phase, (c) the central temperature collapse phase, and (d) the final temperature equalization phase.

Good agreement was found between the measured T_e profile evolution and the double-tearing reconnection simulation described above. The fast T_e profile evolution data with a 2 μsec time resolution are obtained from the two 20-channel grating polychromator ECE arrays [4]. The channel-to-channel separation is about 5–6 cm. The radial spatial resolution for each channel is about 3 cm. The two ECE arrays are toroidally separated by 126°, Fig. 5(a). For $m = 2$ modes, they are effectively simultaneously measuring two T_e profiles separated 63° poloidally. Therefore, if one of the ECE arrays happens to catch the crash phase around the O-point region of the cold island (cf. the 90° section in Fig. 4), the other ECE array will measure the T_e profile near the central region of the hot island (around the 0° section in Fig. 4). The evolution of the second core-crash sawtooth in Fig. 1 is shown in Figs. 5(c)–5(f). Since the crash phase is much shorter ($\lesssim$30 μsec) than the precursor oscillation period ($\gtrsim$2.5 msec), the two ECE arrays measure the sawtooth crash with nearly fixed phase with respect to the island locations. Before the sawtooth precursor, the T_e profiles from both ECE arrays are nearly identical. Just before the crash [$t = t_1$ in Figs. 5(c) and 5(d)], a flat spot with $T_e \sim 3.8$ keV starts to form and expand. It locates at the inner $q = 2$ surface according to the q profile in Fig. 5(b), which indicates that the ECE2 is measuring the hot island region [cf. 0° profile of Fig. 4(a)]. During the crash phase, the hot island grows rapidly outward to the outer $q = 2$ region. The central T_e also starts to drop, see the t_2 profile in Fig. 5(d) and compare with Fig. 4(b). As the reconnection continues to the core, the central T_e collapses. The T_e profile from ECE2 becomes hollow, as predicted by the simulation, see the t_3 profile in Fig. 5(d) and compare with Fig. 4(c). After the crash, the T_e profile starts to flatten, see the t_4 profile in Fig. 5(d) and compare with Fig. 4(d). The T_e evolution from the ECE1 array shows a very different pattern with respect to ECE2. As shown in Figs. 5(e) and 5(f), a 2 keV cold island develops at the outer $q = 2$ surface. The T_e profiles in each stage

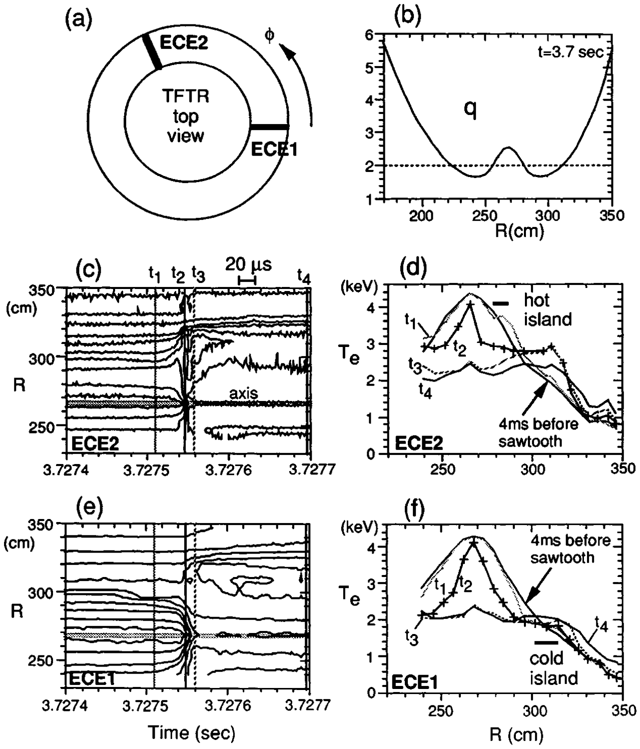

FIG. 5. (a) The two ECE systems are toroidally separated by 126°. (b) The q profile before the second core-crash sawtooth in the discharge shown in Fig. 1. The T_e contour plot (c) and profiles (d) show the T_e evolution measured from the ECE2 array. The T_e evolution in the same time window measured from the ECE1 array is shown in (e) and (f). The basic feature is that the hot island moves out and the cold island moves in, which is in good agreement with the numerical simulation (cf. Fig. 4).

agree well with the simulation shown as the 90° section in Fig. 4. In annular-crash cases, similar good agreement on the T_e evolution has also been found between the ECE measurement and the double-tearing simulation.

Experimentally, we also observed cases where large magnetic islands remain after a fast crash phase followed by a strong $2/1$ postcursor. This phenomenon may be understood from the double-tearing model if the fast reconnection is incomplete. For example, the fast reconnection stops at phase (b) in Fig. 4.

Occasionally, off-axis sawteeth with a $m/n = 3/1$ island precursor are observed in RS plasmas. They happened as $q_{\min}$ passed 3.

Identification of the two magnetic islands in the precursor is usually difficult. This is due mainly to the finite spacing (5–6 cm) between the ECE channels and the very different spatial structure of the double-tearing perturbation. Numerical simulation shows that the δT_e phase inversion feature, which is usually used to identify magnetic islands, becomes very weak in the double-tearing case. Nevertheless, the δT_e phase inversions on both $q = 2$ surfaces were observed when islands were large, as in Fig. 2(b). In higher-β RS/ERS discharges, the double-tearing reconnection mechanism studied here sometimes causes disruptions.

As in $q = 1$ sawtooth studies, two major questions remain to be answered. First, How does the measured q profile change after the sawtooth? Ongoing improvements to the MSE diagnostic and analysis techniques may allows this question to be answered in the future. Second, How is the double-tearing mode destabilized? A statistical data analysis shows that off-axis $2/1$ sawteeth occurred in nearly half the discharges in TFTR RS experiments during the 1995 run. In many cases the discharges with and without sawteeth are very similar in terms of the measured plasma parameters, including $q(r)$. Statistical data from local density and temperature and their gradients show no clear "parameter boundary" between the sawtoothing and nonsawtoothing discharges.

In conclusion, off-axis sawteeth have been observed in TFTR reversed shear experiments. They usually have $m/n = 2/1$ MHD precursors and occur after $q_{\min}$ crosses 2. The crash time ($\sim$20–40 μsec) and repetition time ($\sim$100–400 msec) are similar to the $q = 1$ sawteeth in monotonic q profile plasmas. The stability boundary of the mode is yet to be identified. However, the detailed comparison between the T_e profile evolution and the MHD simulation confirms, for the first time, that the observed off-axis sawteeth are due to the double-tearing magnetic reconnection process.

The authors would like to acknowledge the support and useful discussions with J. Manickam, R. Goldston, R. J. Hawlyruk, W. Stodiek, L. Zakharov, and G. Hoang (Tore-Supra). This research is sponsored by the U.S. Department of Energy under Contract No. DE-AC02-76-CHO-3073.

[1] F. M. Levinton *et al.*, Phys. Rev. Lett. **75**, 4417 (1995).
[2] F. M. Levinton *et al.*, Rev. Sci. Instrum. **63**, 5157 (1992).
[3] R. V. Budny, Nucl. Fusion **34**, 1247 (1994), and references therein.
[4] A. Janos *et al.*, Rev. Sci. Instrum. **66**, 668 (1995).
[5] B. B. Kadomtsev, Fiz. Plazmy **1**, 710 (1975) [Sov. J. Plasma Phys. **1**, 389 (1975)].
[6] R. B. White, D. A. Monticello, M. N. Rosenbluth, and B. V. Waddell, *Plasma Physics and Controlled Nuclear Fusion Research 1977* (IAEA, Vienna, 1977), Vol. 1, p. 569.
[7] B. Carreras, H. R. Hicks, and B. V. Waddell, Nucl. Fusion **19**, 583 (1979).
[8] W. Park, D. A. Monticello, E. Fredrickson, and K. McGuire, Phys. Fluids B **3**, 507 (1991).
[9] W. Park, D. A. Monticello, H. Strauss, and J. Manickam, Phys. Fluids **29**, 1171 (1986).
[10] E. N. Parker, J. Geophys. Res. **62**, 509 (1957).
[11] W. Park, D. A. Monticello, and R. B. White, Phys. Fluids **27**, 137 (1984).
[12] J. F. Drake, R. G. Kleva, and M. E. Mandt, Phys. Rev. Lett. **73**, 1251 (1994).